Electronic Supplementary Material (ESI) for Journal of Materials Chemistry A.

Supporting Information

Interfacial study of clathrates confined in reversed silica pores

Paulo G. M. Mileo[a], Sven M. J. Rogge[a], Maarten Houlleberghs,[b] Eric Breynaert,[b]
Johan A. Martens,[b] and Veronique Van Speybroeck*[a]

[a] Center for Molecular Modeling, Ghent University,
Tech Lane Ghent Science Park Campus A, Technologiepark 46, B-9052 Zwijnaarde, Belgium

[b] Center for Surface Chemistry and Catalysis, Katholieke Universiteit Leuven,
Celestijnenlaan 200F, 3001 Heverlee, Belgium

*Corresponding authors: Veronique.VanSpeybroeck@UGent.be

Further computational details

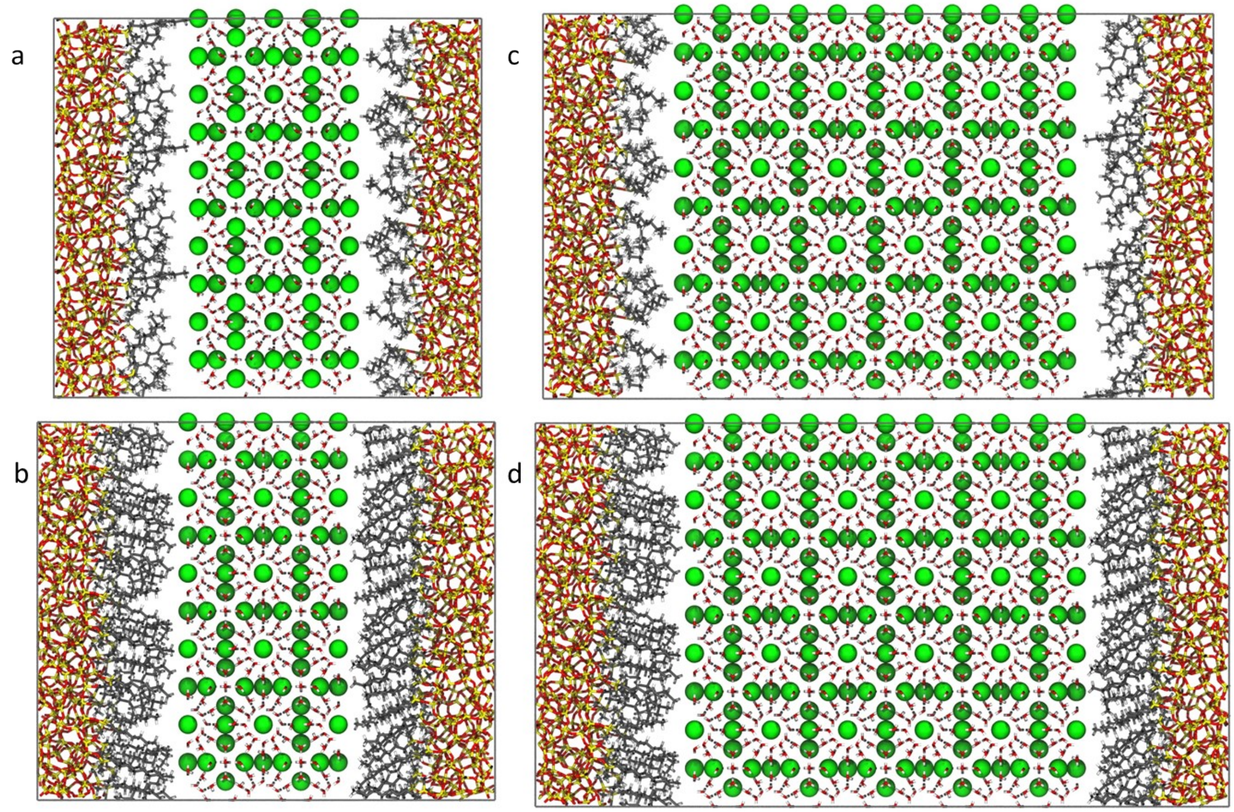

Figure S1. Microscopic representations of non-optimized SiO_2-C_8 models *sp-ld* (a), *sp-hd* (b), *lp-ld* (c) and *lp-hd* (d) with a structure I CH_4 clathrate introduced in their void zones. Same atom color code as in Figure 2 in the manuscript.

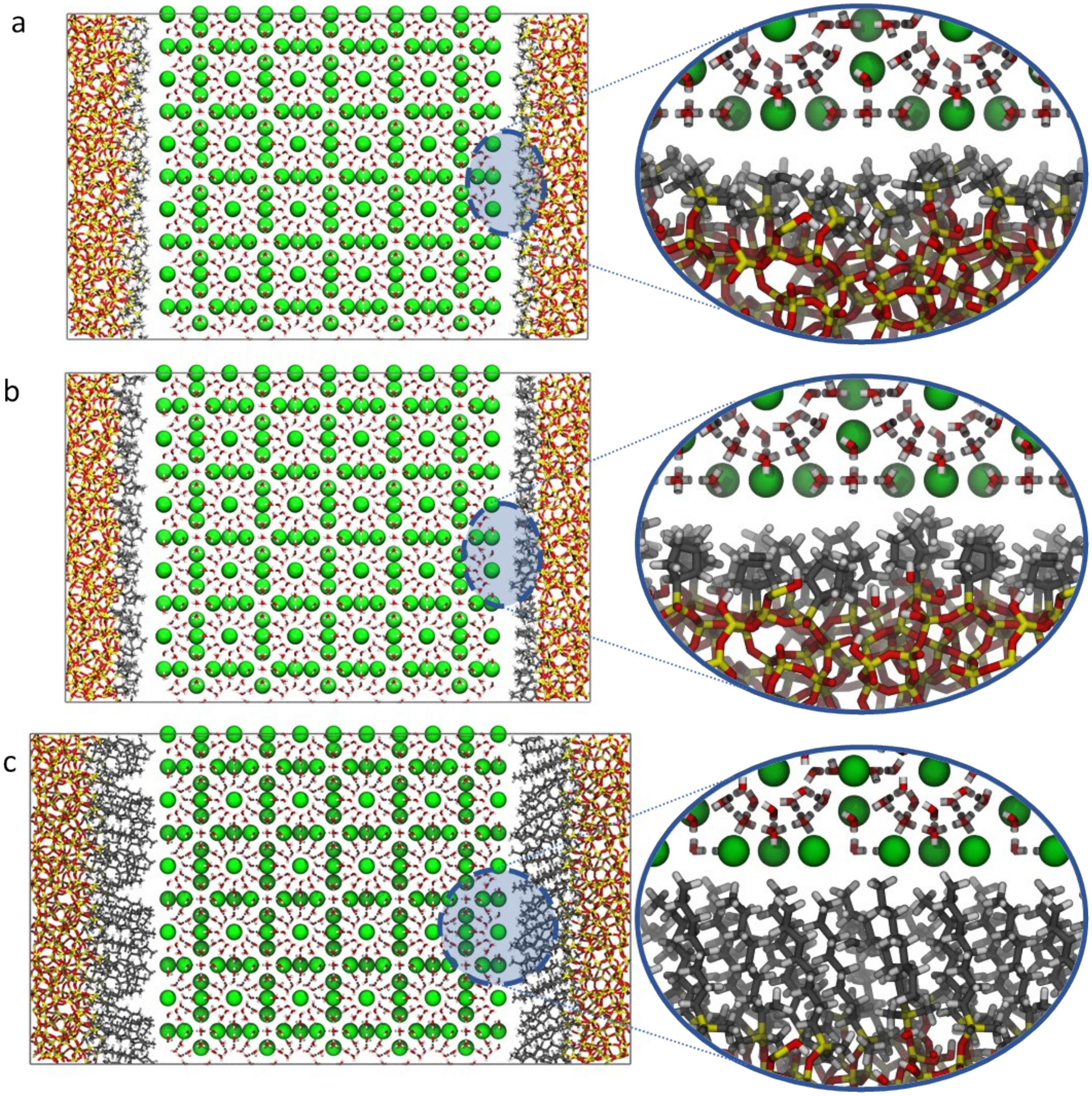

Figure S2. Representation of the microscopic models SiO_2-C_1 (a), SiO_2-cC_5 (b), and SiO_2-C_8 (c) models with a structure I CH_4 clathrate introduced in their void zones. On the right-hand side, a zoom displaying the interface between the alkyl ligands and the clathrate network for each model. Same atom color code as in Figure 2 in the manuscript.

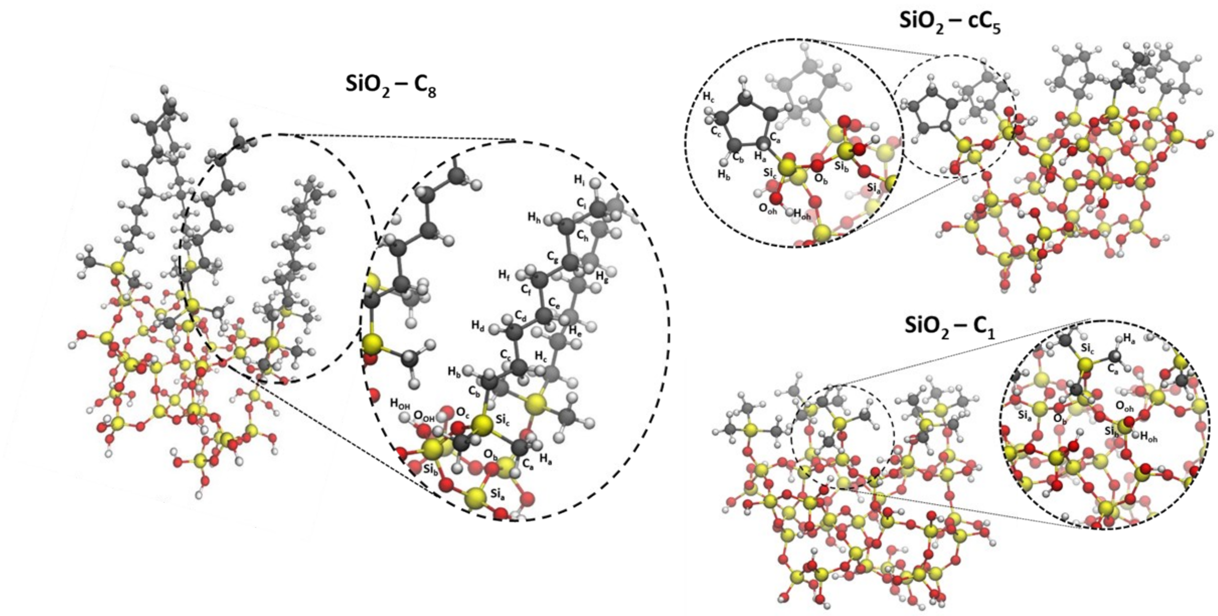

$SiO_2 – C_8$				$SiO_2 – cC_5$		$SiO_2 – C_1$	
Atom type	**Charge (e)**	**Atom type**	**Charge (e)**	**Atom type**	**Charge (e)**	**Atom type**	**Charge (e)**
C_a	-0.6173	H_d	0.0354	C_a	-0.1071	C_a	-0.6328
C_b	-0.2207	H_e	0.0315	C_b	0.0495	H_a	0.1249
C_c	-0.2116	H_f	0.0571	C_c	-0.0276	H_{OH}	0.4282
C_d	0.0075	H_g	0.0585	H_a	0.0120	O_b	-0.7342
C_e	-0.0222	H_h	-0.0167	H_b	-0.0060	O_c	-0.6885
C_f	-0.1947	H_i	0.0978	H_c	-0.0019	O_{OH}	-0.7628
C_g	-0.1318	O_{OH}	-0.6727	H_{OH}	0.4359	Si_a	1.4989
C_h	0.2166	O_b	-0.7214	O_b	-0.7345	Si_b	1.3368
C_i	-0.4336	O_c	-0.6616	O_{OH}	-0.7742	Si_c	1.0299
H_{OH}	0.3320	Si_a	1.4526	Si_a	1.5027		
H_a	0.1310	Si_b	1.3566	Si_b	1.3976		
H_b	0.0560	Si_c	0.9200	Si_c	0.9991		
H_c	0.0560						

Figure S3. Representative cluster models cleaved from the SiO_2-C_8, SiO_2-cC_5 and SiO_2-C_1 microscopic representations with their respective atom types (top) and corresponding DFT-derived partial atomic charges (bottom). Same atom color code as in Figure 2 in the manuscript.

Table S1. Methane storage capacity of the models discussed in this work in terms of mass of methane per total volume.

Structure model	Methane capacity (mg CH_4/cm^3)
SiO_2-C_8 *sp-ld*	60.72
SiO_2-C_8 *sp-hd*	51.36
SiO_2-C_8 *lp-ld*	91.63
SiO_2-C_8 *lp-hd*	82.85
SiO_2-C_1	97.24
SiO_2-cC_5	94.73
SiO_2	93.89

The Orientational Tetrahedral Order (OTO)[1] parameter was calculated using the order[2] python script. This parameter (q) is calculated by averaging the angles formed by the four closest water oxygen neighbors (see Figure 3a in the main text), according to the equation below:

$$q = 1 - \frac{3}{8}\sum_{j=1}^{3}\sum_{k=j+1}^{4}\left(\frac{1}{3} + cos\beta_{ijk}\right)^2 \qquad \text{Equation S1}$$

Herein, β_{ijk} is the angle formed between a central oxygen atom i and two neighboring oxygen atoms j and k.

The mean squared displacements were calculated using a multiple time origin approach and plotted as a function of time.

Analysis of system equilibrium

In order to demonstrate that a simulation time of 10 ns is sufficient to achieve equilibrium at the solid-clathrate interface at 260 K and 60 bar, we carried out 100ns-long MD calculations at these same conditions using the SiO_2-cC_5 and SiO_2-C_8(*sp-ld*) models. As seen in the manuscript, these models respectively showed the lowest and highest degree of disruption of the clathrate matrix. Afterwards, we compared the H_2O microscopic organization and the CH_4 mobility at the interfacial region defined in the manuscript obtained with such simulations with our previous 10ns-long calculations by respectively analyzing donor-acceptor (O_W-O_W) radial distribution functions and self-diffusion coefficients (D_{O_w}) obtained from mean square displacements using the Einstein equation (Equation S2).

$$\lim_{t\to\infty} \left\langle \| r_i(t) - r_i(0) \|^2 \right\rangle_{i \in O_w} = 6 D_{O_w} t \qquad \text{Equation S2}$$

As revealed in the donor-acceptor RDFs of Figure S4, the water organization in the first and second solvation shells is strictly the same in 10ns- or 100ns-long simulations in both models.

We can observe from Figure S5 that also the CH_4 self-diffusion coefficients in the SiO_2-C_8(*sp-ld*) and SiO_2-cC_5 models are very similar either in 10ns- or 100ns-long calculations, with only marginal deviations which may be attributed to the usual numerical errors inherent to diffusivity calculations from mean square displacements.

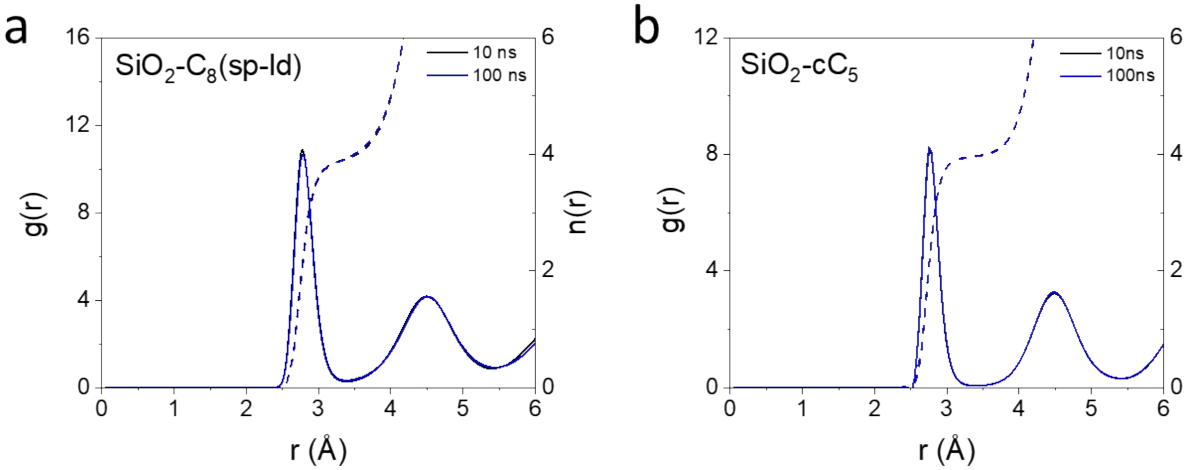

Figure S4. Water donor-acceptor radial distribution functions (solid lines, left Y axis) and their respective integration (dashed lines, right Y axis) obtained from MD calculations carried out for 10 ns (black lines) and 100 ns (blue lines) in the molecular models SiO_2-C_8(*sp-ld*) (a) and SiO_2-cC_5 (b).

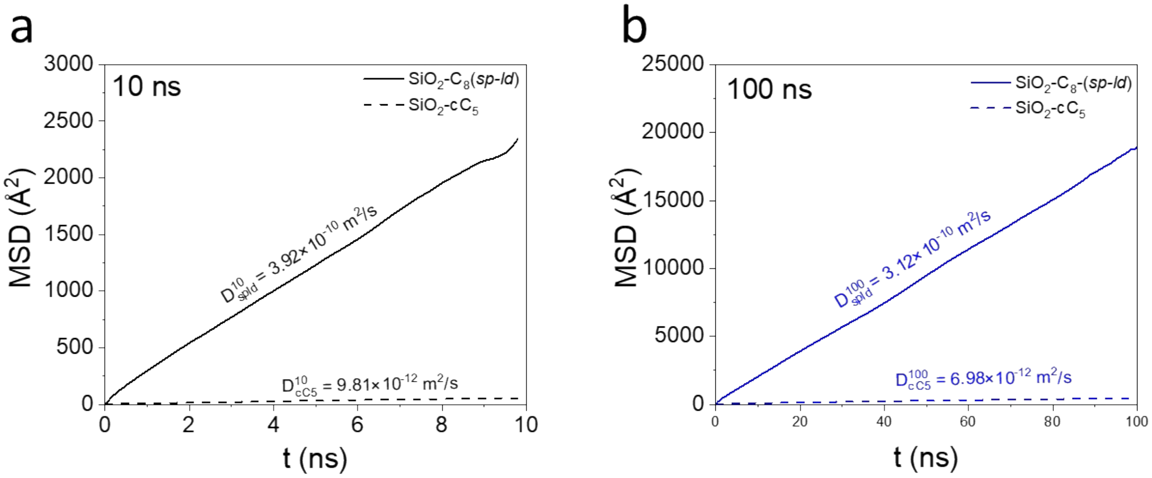

Figure S5. Mean square distances and derived diffusion coefficients obtained from MD calculations carried out for 10 ns (a) and 100 ns (b) in the SiO_2-C_8(*sp-ld*) (solid lines) and SiO_2-cC_5 (dashed lines) models.

As discussed in the manuscript, the interfacial water structuration and methane mobility are very representative parameters to the description of the organizational degree of the clathrate matrix adjacent to the alkyl-substituted SiO_2-molecular models. Therefore, as these parameters are kept the same either at 10 or 100 ns, we are confident that the equilibrium of the evolution of a clathrate phase near the interfaces reported in the manuscripts is well reproduced with a simulation time of 10 ns.

Results

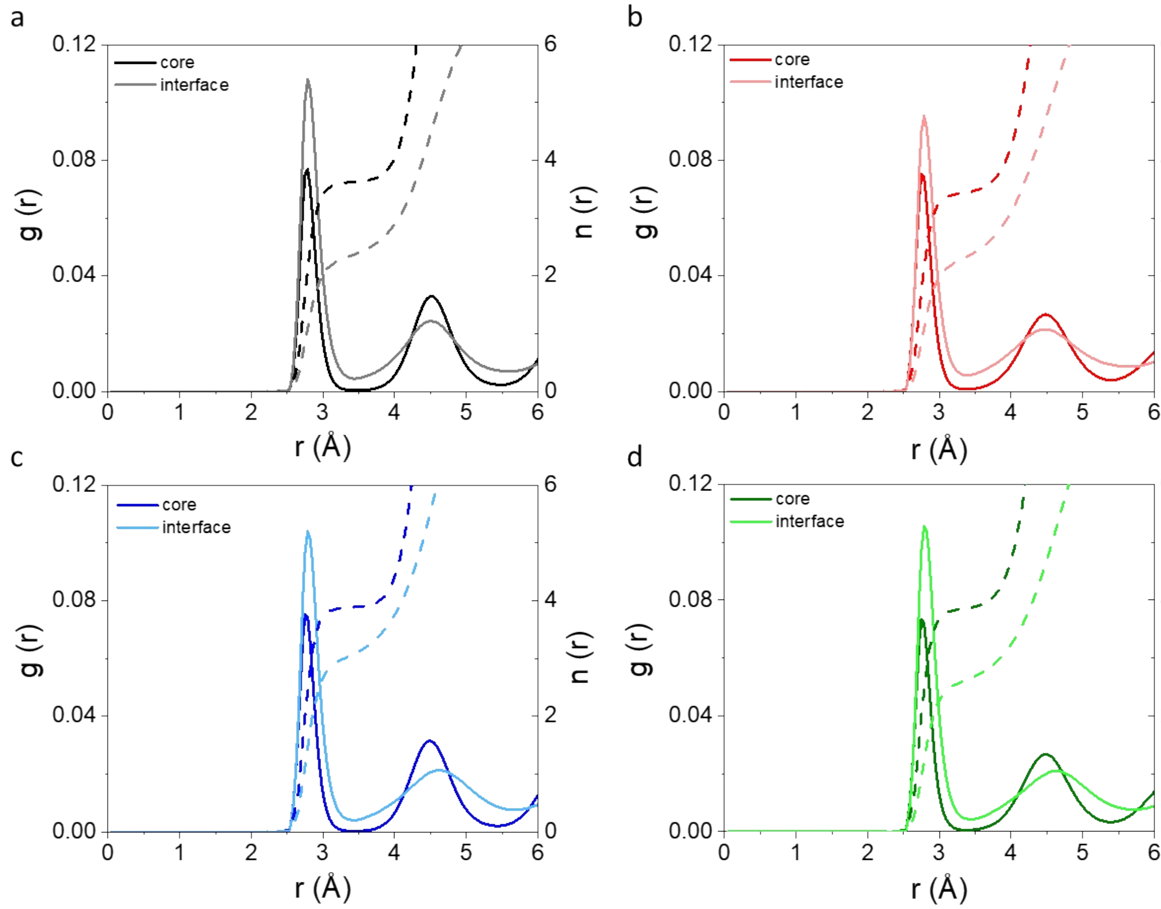

Figure S6. Donor-acceptor radial distribution functions (solid lines) and the corresponding cumulative distribution functions (dashed lines) obtained from the water molecules located at the core of the clathrate phases (dark colors) and at their interface (light colors) of the SiO_2-C_8 slabs on the sp-hd (a), sp-ld (b), lp-hd (c), lp-ld (d) configurations.

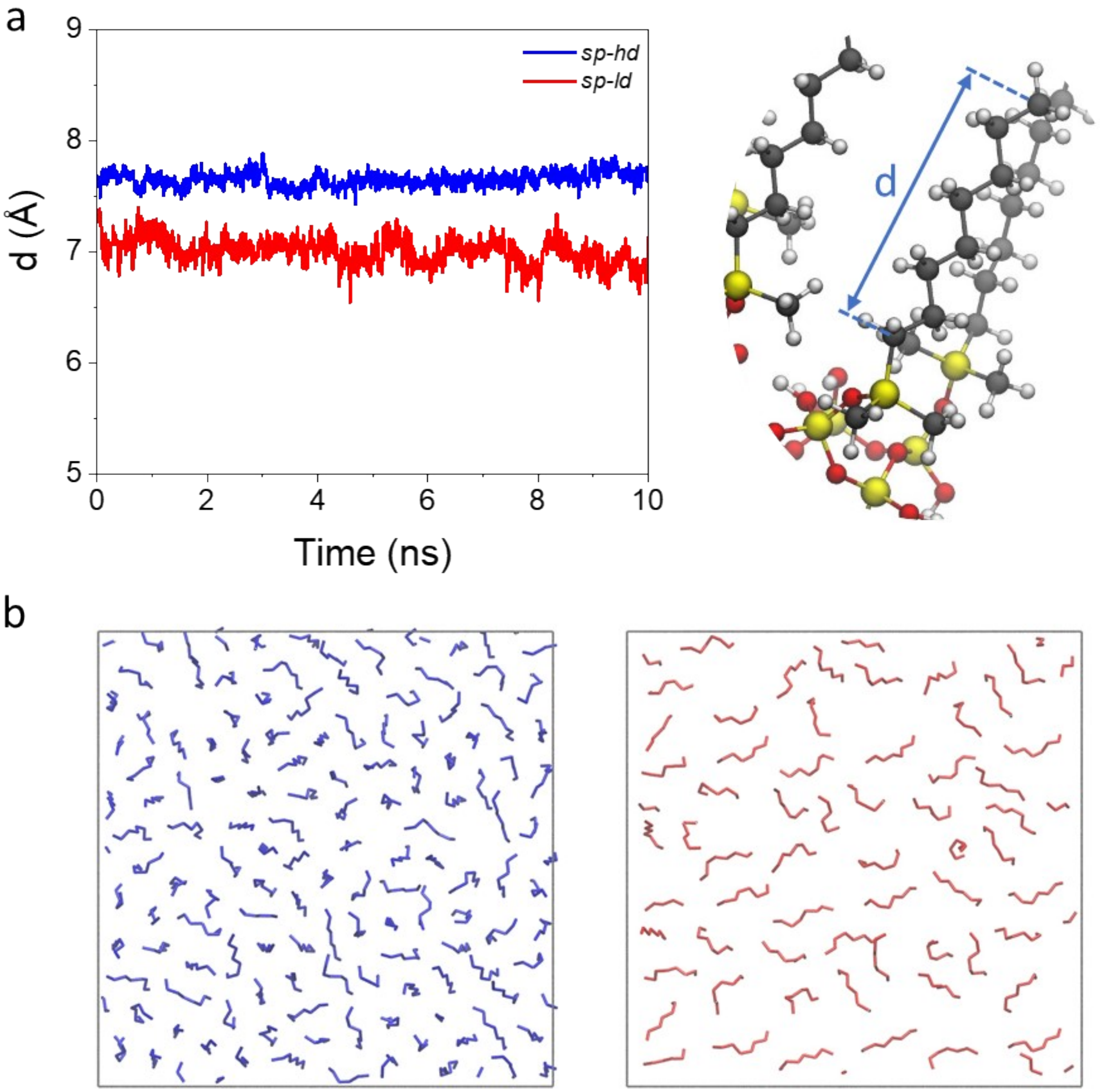

Figure S7. (a) Comparison of end-to-end distances of octyl chains in structure models *lp-hd* (blue line) and *lp-ld* (red line). (b) Top view parallel with the *z*-direction of surfaces of *lp-hd* (right) and *lp-ld* (left) configurations displaying the orientations of the alkyl chains. While in the former they are mostly perpendicular with respect to the plane, in the latter these chains are mostly tilted to the point of being parallel to the surface.

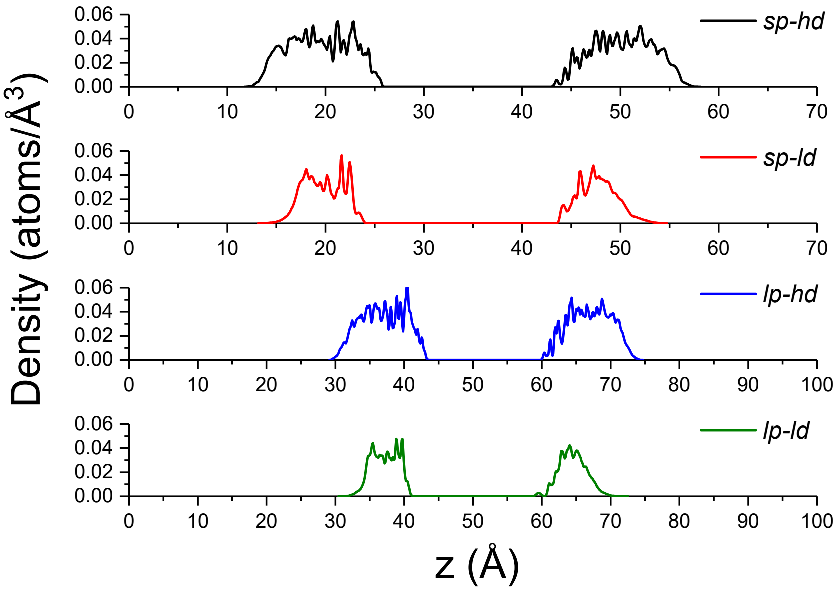

Figure S8. Density plots of the carbon atoms in the SiO_2-C_8 octyl chains of the *sp-hd* (a), *sp-ld* (b), *lp-hd* (c), and *lp-ld* (d) configurations.

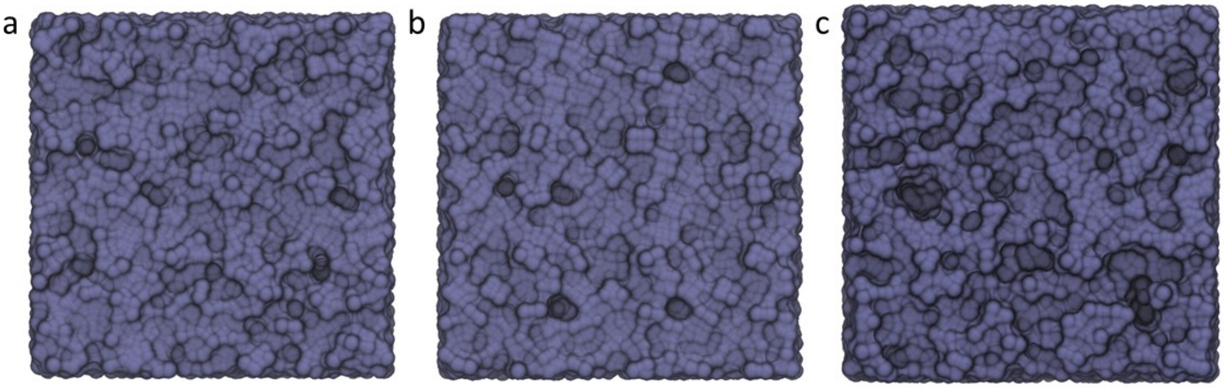

Figure S9. Contour surface plots displaying the surface topology of structure models SiO_2-C_1 (a), SiO_2-cC_5 (b) and SiO_2-C_8 (c) obtained from the VMD software.[3]

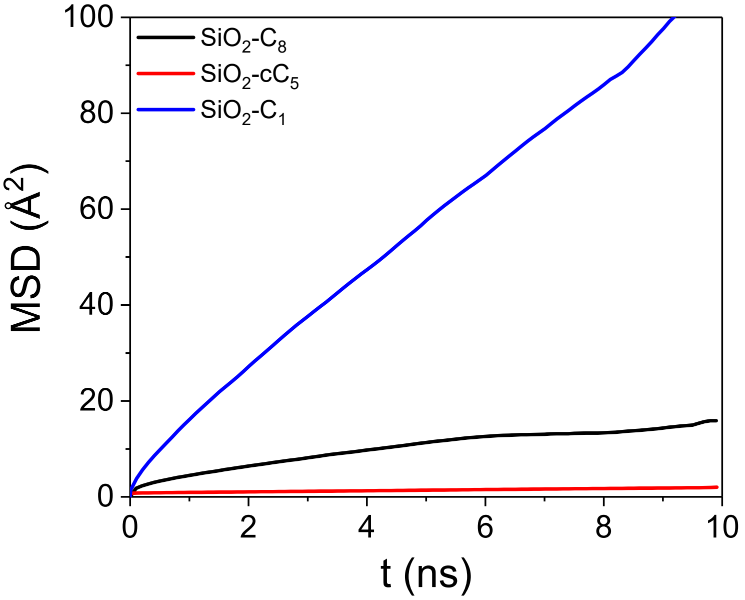

Figure S10. Mean square displacement of CH_4 molecules at the clathrate/pore wall interface in the SiO$_2$-C$_1$ (black line), SiO$_2$-cC$_5$ (red line) and SiO$_2$-C$_8$ (blue line) models.

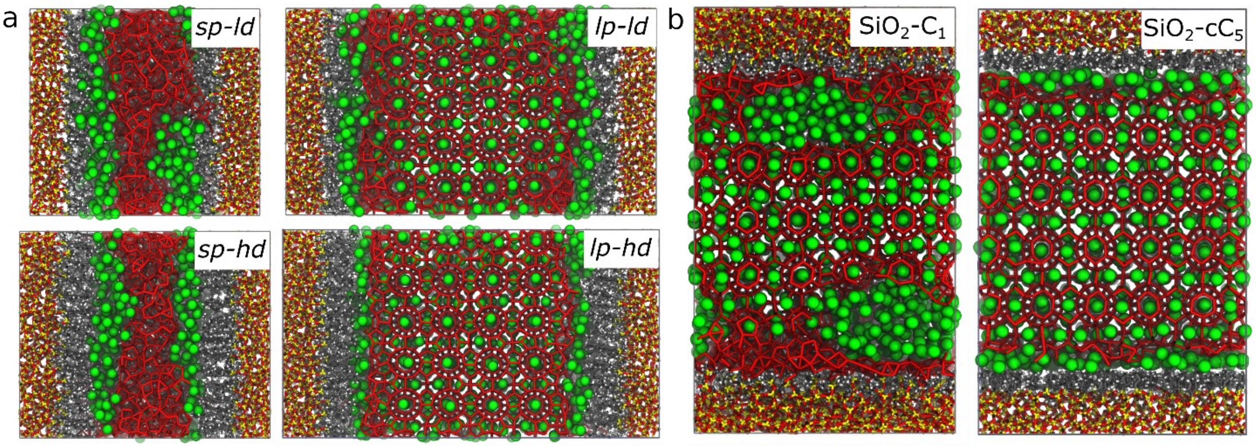

Figure S11. Representative snapshots showing confined clathrate configurations after 10 ns long MD calculations at 60 bar and 300 K on SiO$_2$-C$_8$ structure models *sp-ld*, *sp-hd*, *lp-ld* and *lp-hd* (a) and on SiO$_2$-C$_1$ and SiO$_2$-cC$_5$ structure models (b). Same atom color code as in Figure 2 in the manuscript.

Supporting references

1 E. Duboué-Dijon and D. Laage, *J. Phys. Chem. B*, 2015, **119**, 8406–8418.

2 P. Du and V. K. S. S. Don, iOrder, 2018.

3 W. Humphrey, A. Dalke and K. Schulten, *J. Mol. Graph.*, 1996, **14**, 33–38.